

Characterization of surface roughness of Pt Schottky contacts on quaternary n-Al_{0.08}In_{0.08}Ga_{0.84}N thin film assessed by atomic force microscopy and fractal analysis

Ștefan Țălu · Alaa J. Ghazai · Sebastian Stach ·
Abu Hassan · Zainuriah Hassan · Mihai Țălu

Received: 31 August 2013 / Accepted: 8 November 2013 / Published online: 20 November 2013
© Springer Science+Business Media New York 2013

Abstract The purpose of this study was to analyze surface topography of Pt Schottky contacts on quaternary n-Al_{0.08}In_{0.08}Ga_{0.84}N thin film. To understand how the effect of temperature changes the layers surface, the surface topography was characterized through atomic force microscopy (AFM) and fractal analysis. Pt Schottky contacts grown on nanostructure Al_{0.08}In_{0.08}Ga_{0.84}N thin film grown by molecular beam epitaxy technique on sapphire substrate at annealing temperatures range of 300–500 °C were used. AFM analysis was performed in contact mode, on square areas of 10 × 10 μm², by using a Nanosurf

Easyscan 2 AFM system. Detailed surface characterization of the surface topography was obtained using statistical parameters of 3D surface roughness, according with ISO 25178-2: 2012, provided by the AFM software. The results revealed that the high quality Schottky contact with the Schottky barrier heights and ideality factor of 0.76 and 1.03 respectively can be obtained under 30 min annealing at 400 °C in N₂ ambience. The surface roughness of Pt Schottky contacts on quaternary n-Al_{0.08}In_{0.08}Ga_{0.84}N thin film revealed a fractal structure at nanometer scale. Results obtained by fractal analysis confirm the relationship between the value of the fractal dimension and the statistical surface roughness parameters. AFM and fractal analysis are accurate tools that may assist manufacturers in developing Pt Schottky contacts on quaternary n-Al_{0.08}In_{0.08}Ga_{0.84}N thin film with optimal surface characteristics and provides different yet complementary information to that offered by traditional surface statistical parameters.

Ș. Țălu (✉)

Department of AET, Discipline of Descriptive Geometry and Engineering Graphics, Faculty of Mechanical Engineering, Technical University of Cluj-Napoca, 103-105 B-dul Muncii St., 400641 Cluj-Napoca, Cluj, Romania
e-mail: stefan_ta@yahoo.com

A. J. Ghazai

Nassiriya Nanotechnology Research Laboratory (NNRL), Physics Department, Science College, Thi-Qar University, 00964 Nassiriya, Thi Qar, Iraq

S. Stach

Department of Biomedical Computer Systems, Faculty of Computer Science and Materials Science, Institute of Informatics, University of Silesia, ul. Będzińska 39, 41-205 Sosnowiec, Poland

A. Hassan · Z. Hassan

Nano-Optoelectronics Research and Technology Laboratory, School of Physics, Universiti Sains Malaysia, 11800 Penang, Malaysia

M. Țălu

Department of Applied Mechanics, Faculty of Mechanical Engineering, University of Craiova, 165 Calea București St., 200585 Craiova, Dolj, Romania

1 Introduction

In the last years of the 20th decade, group III-nitride materials, especially quaternary AlInGaN, have received considerable attention for their excellent electrical and optical properties, as well as their possible integration with current electronic and optoelectronic devices [1].

These materials can operate under the harshest circumstances, such as at high temperature and high power, making them promising candidates in the electronic and optoelectronic device area. These materials possess wide band gap energy, high breakdown field, and high electron saturation velocity, which make them promising candidates for operation at high temperature, high power, and high frequency [2].

Most researchers in this field have been interested in and have focused on studying the effect of Pt contact thermal annealing on binary GaN and ternary AlGaN [3–9]. However, the literature regarding Pt contacts on n-GaN is not fully understood, and few reports discuss the thermal annealing effect on quaternary AlInGaN.

Thermal annealing temperature effects on the electrical and structural properties of platinum/molybdenum (Pt/Mo) Schottky contacts on an n-type GaN have been investigated by Rajagopal et al. [3] using current–voltage (I–V), capacitance–voltage (C–V), X-ray diffraction (XRD), and X-ray photoelectron spectroscopy techniques. They concluded that Pt/Mo contact does not seriously suffer from thermal degradation during the annealing process even at 600 °C [root mean square (RMS) roughness of 5.41 nm].

Wang et al. [4] studied the structural evolution and temperature dependence of the Schottky barrier heights (SBHs) of Pt contacts on n-GaN epilayer at various annealing temperatures by Rutherford backscattering spectrometry, X-ray diffraction measurements, Auger electron spectroscopy, scanning electron microscopy and current–voltage measurements and reported the degradation of Pt contacts on n-GaN above 600 °C.

Yu et al. [5] have reported that the SBH, which is effective at room temperature, was 0.79 eV for Ir/Pt on GaN.

The dark current characteristics of thermally treated contacts on GaN-based ultraviolet photo detectors and the thermal stability of the contacts at various annealing temperatures (300–700 °C) have been investigated by Lee et al. [6].

Reddy et al. [7] have studied the electrical and structural properties of palladium/molybdenum Schottky contacts on n-type GaN with respect to annealing temperature using I–V, C–V, XRD, and AES techniques, and no significant degradation was observed in the surface morphology (RMS roughness of 4.61 nm) of the contact even after annealing at 600 °C.

A comprehensive, up-to-date compilation of band parameters for the technologically important III–V zinc blende and wurtzite compound semiconductors, namely, GaAs, GaSb, GaP, GaN, AlAs, AlSb, AlP, AlN, InAs, InSb, InP, and InN, along with their ternary and quaternary alloys, has been studied by Vurgaftman et al. [8].

The application of thermal annealing treatment to Pt/Al_{0.08}In_{0.08}Ga_{0.84}N metal–semiconductor contacts at various annealing temperatures (300–600 °C) has been reported by Ghazai et al. [9]. They conclude that RMS, better surface morphology, and high SBH were obtained for Pt/Al_{0.08}In_{0.08}Ga_{0.84}N contacts annealed at 400 °C.

Different optical imaging and diffraction techniques have been used extensively to investigate the surface roughness of Pt contact on n-type GaN and ternary AlGaN

because of the growing interest in the electronic and optoelectronic device area and modern manufacturing technology [3–9].

The quantitative characterization of surface morphology of Pt Schottky contacts on n-type GaN and ternary AlGaN thin films is important since many physical and chemical properties, such as electrical, optical, and tribological properties depend on the surface morphology [3, 4, 7, 9].

In the last decades in the area of surface engineering, atomic force microscopy (AFM) have been developed as research useful tool for exploring the surface morphological features [7, 9].

Two main approaches may be distinguished to describe the 3D surface roughness: statistical (the classical descriptive approach) [10, 11] and fractal description (the modern approach) [11–13].

The fractal geometry proposed by B.B. Mandelbrot as modern tool may be used to describe the surface morphology and complexity of irregular microstructures, whose complex geometry cannot be characterized by traditional Euclidean geometry [11, 14].

Fractal methods have been shown to have a strong ability to discriminate profiles measured from different surfaces and can be related to functional models of interactions with surfaces [11].

A fractal description has the potential to considerably simplify the statistical approach and can concisely describe the surface morphology [11, 12, 14, 15]. Furthermore, due to easy implementation, high precision and low computational time, the fractal analyses allow extracting different types of information from complex surface characteristics, in contrast to statistical analyses.

The irregularities of Pt contact on n-type GaN and ternary AlGaN surfaces are not perfectly homogeneously distributed, and effectively differences in 3D surface roughness values have been observed at different magnifications [3, 7, 9].

The topography of 3D surfaces add a new level of understanding to the nanotribology processes, such as adhesion, contact formation, friction of adsorbed layers, seen on a atomic level [16] etc. Also, there is a need for atomic-scale methods in 3D films surfaces investigation and to try to link atomic-scale observations with macroscopic continuum models and experimental results, particularly concerning structure, energetics, dynamics, transport and thermodynamics processes.

The purpose of this study is to characterize the 3D surface topography of Pt Schottky contacts on quaternary n-Al_{0.08}In_{0.08}Ga_{0.84}N thin film, through AFM and fractal analysis. We have investigated Pt contact based on its high work function (about 5.65 eV) and high resistance to oxidation and corrosion. To our knowledge, this paper is the first study of the surface roughness assessed by AFM and

fractal analysis of Pt Schottky contacts on $n\text{-Al}_{0.08}\text{In}_{0.08}\text{Ga}_{0.84}\text{N}$ grown on sapphire substrate at various annealing temperatures (400–500 °C). The fractal analysis reveals the existence of self-similar and fractal characteristics in the surface morphologies.

1.1 Fractal theory

Conventionally, a 3D rough surface is assumed to be a random process, to exhibit fractal characteristics, which can be characterized by fractal parameters that are independent of all scale of roughness [11, 12]. The 3D surface topography of thin films possess only statistical self-similarity, which takes place only in the restricted range of the

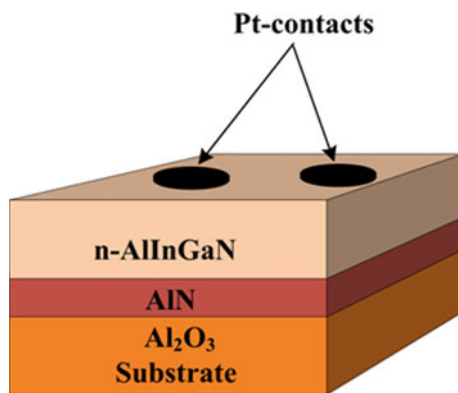


Fig. 1 Pt contacts on $n\text{-Al}_x\text{In}_y\text{Ga}_{1-x-y}\text{N}$ film grown on sapphire substrate

spatial scales [17]. There are different methods of analysing fractal profiles and surfaces [11, 15, 18].

Fractal profiles and surfaces usually have the following characteristics:—they are continuous but nowhere differentiable;—they are not made up of smooth curves, but rather maybe described as lagged or irregular;—they have features that repeat over multiple scales;—they have features that repeat in such a way that they are self-similar with respect to scale over some range of scales [11].

Fractal dimension D_f is a quantitative parameter of a fractal object and describes how the fractal object occupies the metric space to which it belongs [12, 14, 15]. In the case of 3D surfaces, the fractal dimension is an intrinsic property of the surface, which is scale independent. It indicates how much the fractal surface fills the 3D volume and represents the quantitative measure of 3D microstructure complexity [11, 12].

Generally, the fractal dimension D_f of a surface is a non-integer value within the range $2 \leq D_f \leq 3$, where $D_f = 2$ (for ideally smooth surfaces) and $D_f = 3$ (for surfaces with a rough that occupy all available volume) [16].

An increasing value of D_f indicates higher level of fractality, a more irregular shape of the surface roughness. Different studies suggested a correlation between the different surface roughness parameters and the fractal dimension D_f [11, 19].

A 3D rough surface is covered by nanoasperities (nanoscale protrusions and cavities having different geometries) with different orders of size. The distribution of nanoasperities may spread over a region in such a way that small nanoasperities appear almost everywhere,

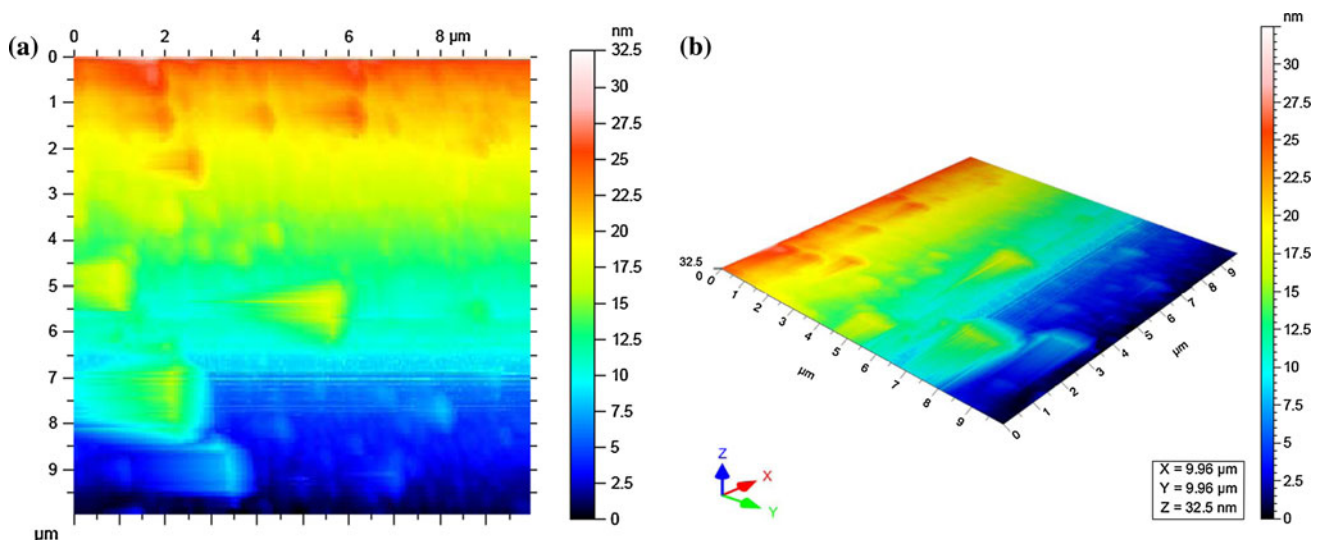


Fig. 2 A representative AFM image of Pt contacts on $n\text{-Al}_{0.08}\text{In}_{0.08}\text{Ga}_{0.84}\text{N}$ film grown on sapphire substrate as deposited. Scanning square area of $10 \times 10 \mu\text{m}$. **a** Microtopographic 2D orthographic

image and **b** microtopographic 3D perspective image. The vertical range of the displayed data (in nanometres [nm]) and the colour bar are shown on the right side of the AFM image

medium nanoasperities exist in many places, and large nanoasperities are concentrated only in a few places.

The fractal analyses depend on the experimental and methodological parameters involved in AFM measurements such as: measurement system, diversity of samples, image acquisition, type of image, image processing, fractal analysis methods including the algorithm and specific calculation used etc. [11, 12, 15, 18].

In our study, for these surfaces the best method of fractal analysis is morfological envelopes [20].

In this method [21] the upper and lower envelopes are calculated by morphological opening and closing using a structuring element which is a horizontal line segment of length ϵ . The graph of the calculated volume for surfaces ($V\epsilon$) is drawn as a function of the scale (size of the structuring elements): $\ln(V\epsilon)/\ln(\epsilon)$. A logarithmic scale is used for the axes, but the values of the graduations are given as dimensional units. The calculated parameters are: fractal dimension, slope (slope of the regression line) and R^2 (correlation coefficient of the regression line). Both of

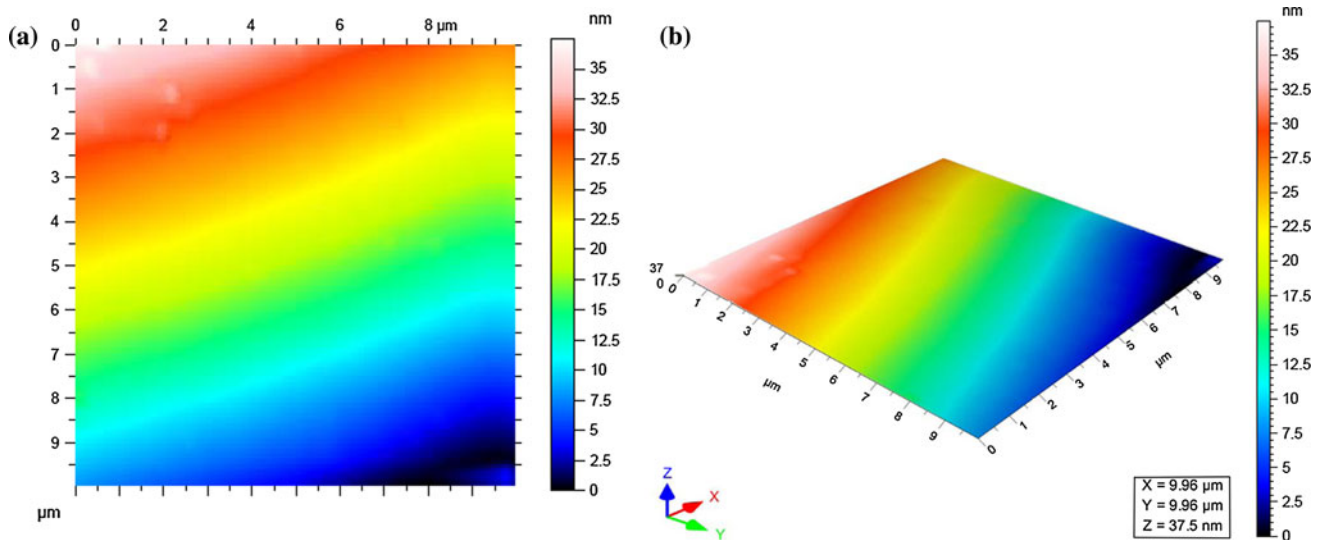


Fig. 3 A representative AFM image of Pt contacts on n-Al_{0.08}In_{0.08}Ga_{0.84}N film grown on sapphire substrate at annealing temperatures of 400 °C. Scanning *square* area of 10 × 10 μm. **a** Microtopographic

2D orthographic image and **b** microtopographic 3D perspective image. The *vertical* range of the displayed data (in nanometres [nm]) and the *colour* bar are shown on the *right* side of the AFM image

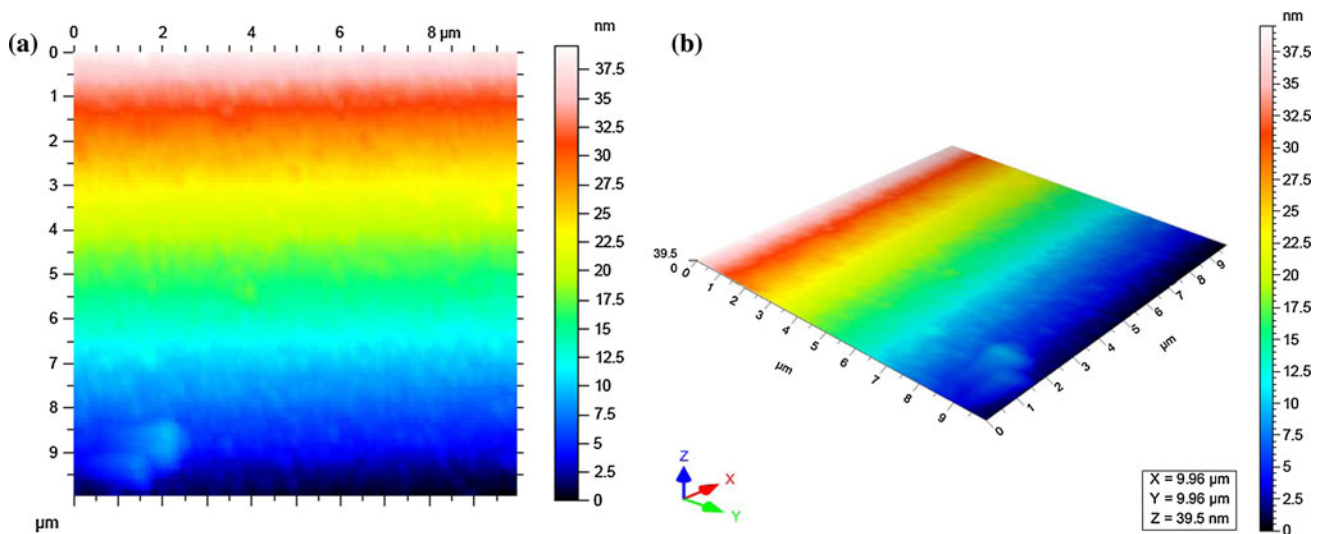


Fig. 4 A representative AFM image of Pt contacts on n-Al_{0.08}In_{0.08}Ga_{0.84}N film grown on sapphire substrate at annealing temperatures of 500 °C. Scanning *square* area of 10 × 10 μm. **a** Microtopographic

2D orthographic image and **b** microtopographic 3D perspective image. The *vertical* range of the displayed data (in nanometres [nm]) and the *colour* bar are shown on the *right* side of the AFM image

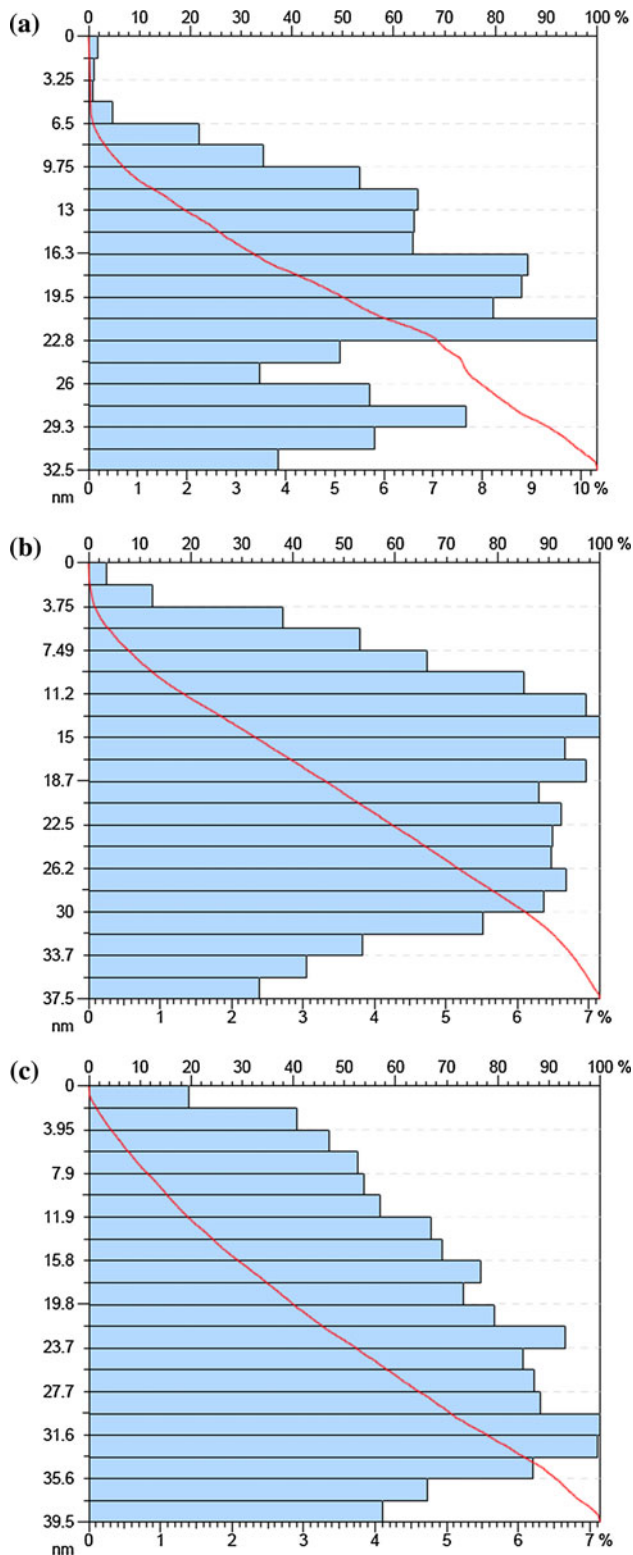


Fig. 5 The depth histogram enables to observe the density of the distribution of the data points on the surface. The vertical axis is graduated in depths: the horizontal axis is graduated in % of the whole population. The Abbott-Firestone curve presents the bearing ratio curve, i.e. for a given depth, the percentage of the material traversed in relation to the area covered. This function is the cumulating function of the amplitude distribution function. The horizontal axis represents the bearing ratio (in %), and the vertical axis represents the depths (in the measurement unit). The Pt contacts on n-Al_{0.08}In_{0.08}Ga_{0.84}N film grown on sapphire substrate: **a** as deposited, **b** after annealing treatment at 400 °C, **c** after annealing treatment at 500 °C

lines that corresponds best (i.e. the one out of the two regression lines whose correlation coefficient is nearer to 1 for a profile and nearer to 2 for a surface).

1.2 Statistical description of 3D surface roughness

Detailed surface characterization was obtained using six quantitative parameters [height, functional, spatial, hybrid, functional (volume) and feature parameters], according with ISO 25178-2: 2012 [22], provided by the AFM software. Detailed information on the objective parameters used to obtain information on the 3D surface roughness is reported in the Appendix.

In our study, the statistical description and the fractal geometry is used to characterize the 3D surface roughness.

2 Materials and methods

2.1 Experimental procedure

The nanostructure Al_{0.08}In_{0.08}Ga_{0.84}N thin film was employed. The nanostructure has a thickness of 100 nm and was grown on sapphire substrate using Plasma Assistance molecular beam epitaxy technique (PA-MBE). The RCA cleaning method was performed at room temperature prior to any fabrication process to remove any contamination on the wafers, such as thin oxide or residual organic residues. The procedure included the use of NH₄OH:H₂O = 1:50 solution for 10 min, after which the samples were washed with deionized water. Subsequently, the samples were dipped into HF: H₂O = 1:50 for 10 s and then washed again with deionized water. The cleaned samples were then chemically etched in boiling HCl: HNO₃ = 3:1 aqua regia for 10 min to reduce the amount of oxygen and carbon contamination on the quaternary AlInGaN surface. The wafers were then blown dry with compressed air after cleaning.

The Schottky contact metals were then deposited on the n-Al_{0.08}In_{0.08}Ga_{0.84}N films using a suitable metal mask with a thickness of 250 nm and a target purity of 99.99 %, which was obtained using the Edwards A500 RF-sputtering system. I–V characteristics were applied to the n-Al_{0.08}In_{0.08}Ga_{0.84}N thin

these parameters are calculated for two regression lines, one connecting the points to the left of the graph, the other connecting the points to the right. The fractal dimension is calculated from the slope of that one of the two regression

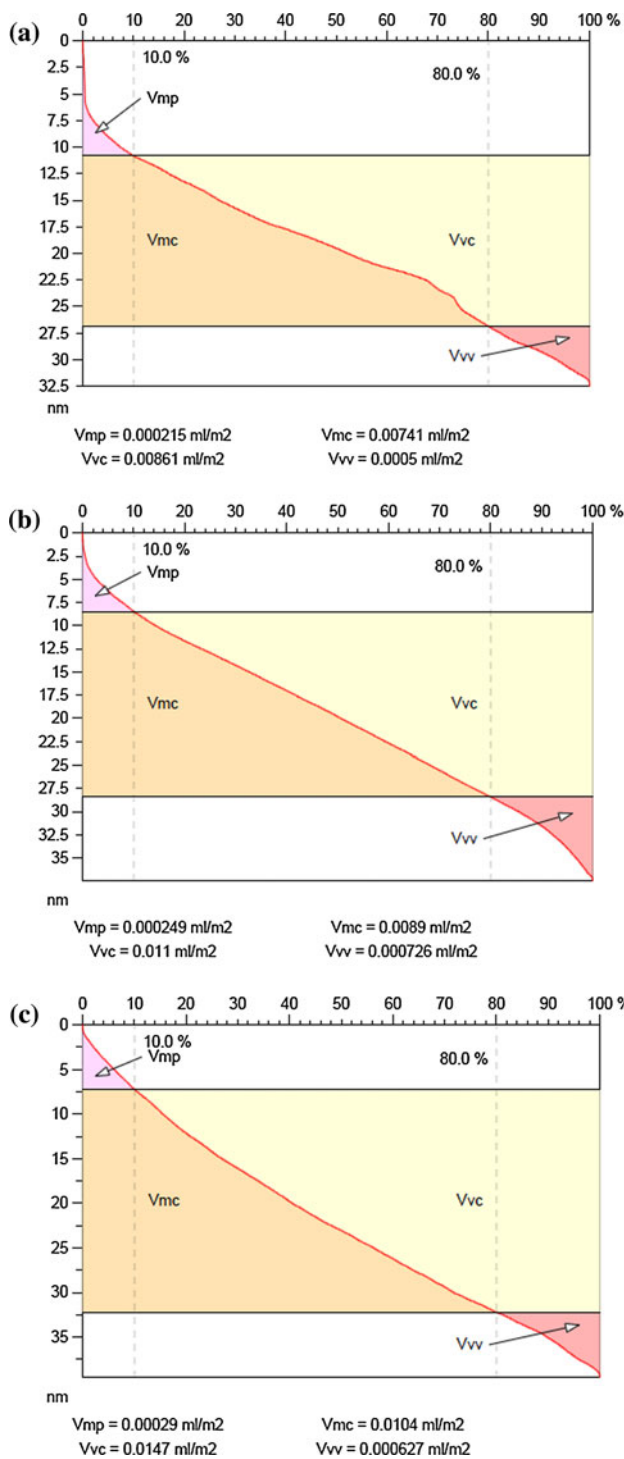


Fig. 6 Graphical study of volume parameters (surface): V_{mp} , V_{vc} , V_{vc} and V_{vv} parameters based upon the Abbott curve calculated on the surface. Two bearing ratio thresholds are defined (using the vertical bars that are drawn with dotted lines). By default, these thresholds are set at bearing ratios of 10 and 80 %. The first threshold, $p1$ (default: 10 %), is used to define the cut level $c1$ (and $p2$ defines $c2$, respectively). The Pt contacts on $n\text{-Al}_{0.08}\text{In}_{0.08}\text{Ga}_{0.84}\text{N}$ film grown on sapphire substrate: **a** as deposited, **b** after annealing treatment at 400 °C, **c** after annealing treatment at 500 °C

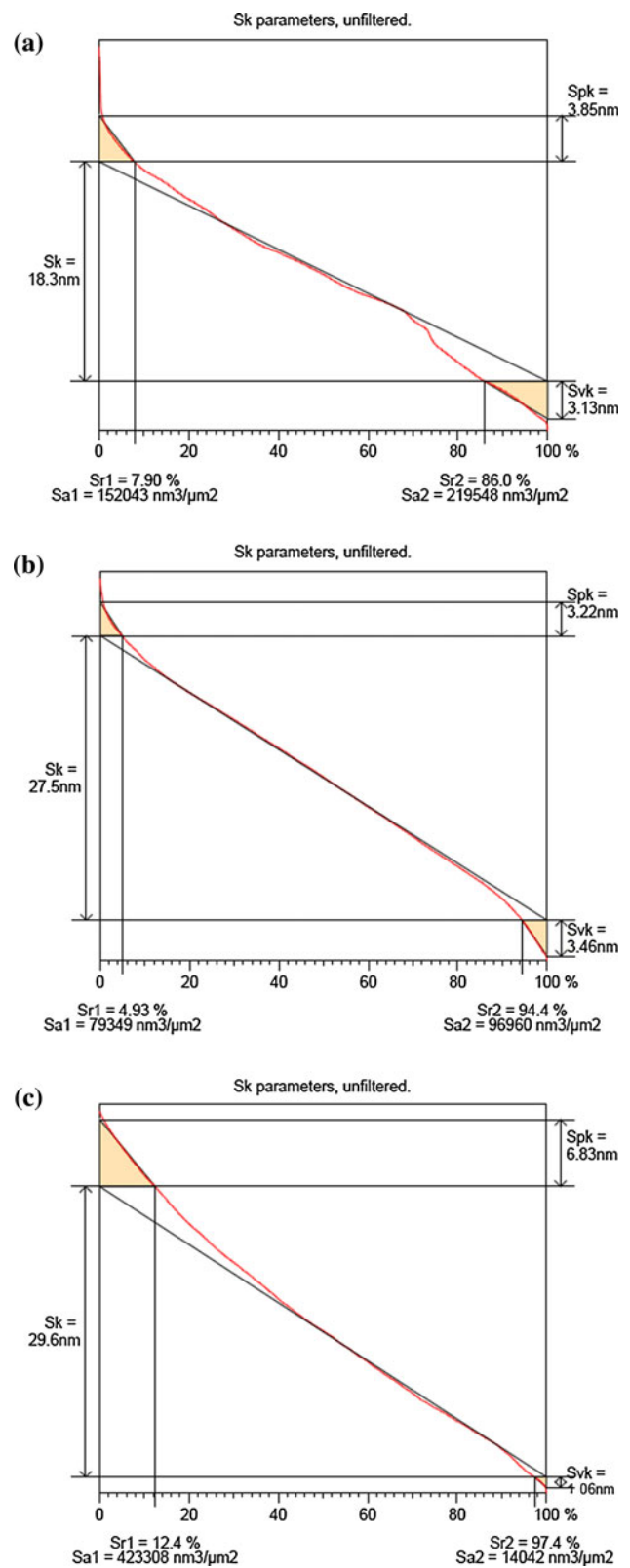


Fig. 7 Graphical study of S_k parameters. The Pt contacts on $n\text{-Al}_{0.08}\text{In}_{0.08}\text{Ga}_{0.84}\text{N}$ film grown on sapphire substrate: **a** as deposited; **b** after annealing treatment at 400 °C; **c** after annealing treatment at 500 °C

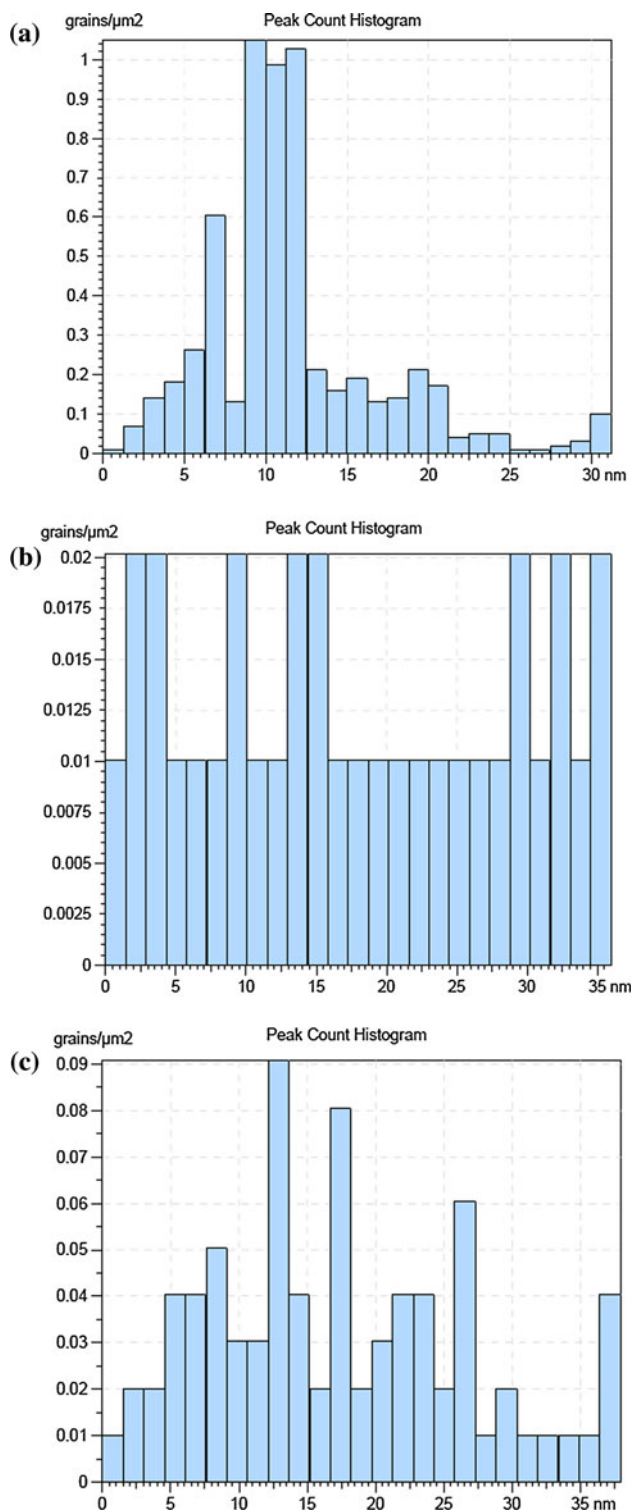


Fig. 8 The *peak* count histogram. The Pt contacts on n-Al_{0.08}In_{0.08}Ga_{0.84}N film grown on sapphire substrate: **a** as deposited, **b** after annealing treatment at 400 °C, **c** after annealing treatment at 500 °C

film, which was grown on sapphire substrate using the LIV Characteristic System Model Optronic Spectroradiometer Lab OL 770-LED. The SBH was then calculated for these samples.

Figure 1 shows the schematic diagram of the Pt contacts on the n-Al_{0.08}In_{0.08}Ga_{0.84}N thin film grown on sapphire (Al₂O₃) substrate.

The high-resolution XRD PANalytical X'pert Pro MRD, with a Cu- α_1 wavelength radiation source equal to 1.5406 Å, was used to identify the structures and crystalline quality of the samples.

The surface morphology was determined using a Nanosurf Easyscan 2 AFM system [23] operating in contact mode and in static force.

The experiments were conducted in the same room at room temperature (23 ± 1 °C) and (50 ± 1 %) relative humidity. Atomic force microscopy (AFM) analysis was performed on square areas measuring 10×10 μm using a Model CL-10 cantilever (Vista Probes Cantilever, USA) [24]. This device is a pyramidal-shaped silicon cantilever with the following nominal specifications: resonant frequency of 12 kHz, spring constant of 0.2 N/m, radius of 2 nm, length of 450 μm, width of 40 μm, and thickness of 2 μm.

All samples were acquired at a scan rate of 1 Hz with an image definition of 256 pixels \times 256 pixels over different square areas. The measurements were repeated three times for each sample on different reference areas to validate the reproducibility of these features. The AFM images were analyzed using scanning probe image processor software [25].

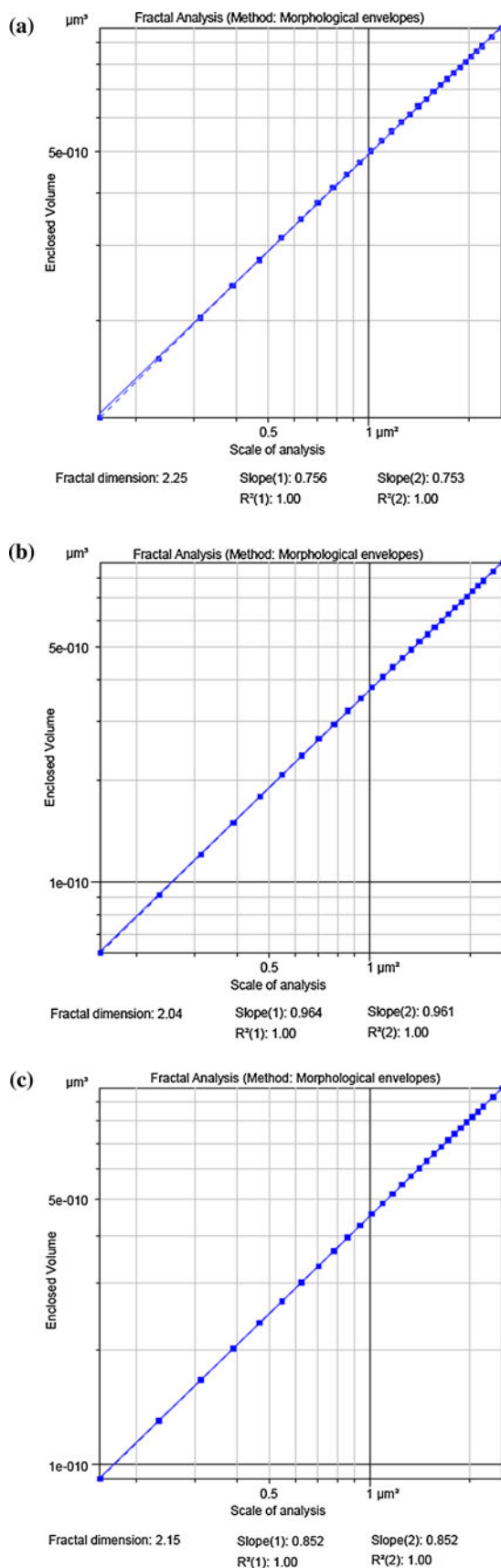
The fractal analyses from the AFM data were made using the proposed fractal analysis method.

2.2 Statistical analysis

Statistical analyses were performed using the GraphPad InStat version 3.20 computer software package (GraphPad, San Diego, CA, USA) [26]. The Kolmogorov–Smirnov test was used to assess the normal distribution of quantitative variables. Comparisons among different areas within the same sample were performed using independent samples *T* test. When statistical significance was found, the difference between two groups was further compared using the Mann–Whitney *U* test. Differences with a *P* value of 0.05 or less were considered statistically significant. The average *D_f* results were expressed as mean value and standard deviation.

2.3 Fractal analysis of surface roughness

An analysis of the stereometric files was conducted based on the original algorithm (in MATLAB software R2012b, MathWorks, Inc.), which consists in fractal scaling (in many approximation steps) of the surface measured with an AFM.



◀ **Fig. 9** Fractal dimension. The Pt contacts on n-Al_{0.08}In_{0.08}Ga_{0.84}N film grown on sapphire substrate: **a** as deposited, **b** after annealing treatment at 400 °C, **c** after annealing treatment at 500 °C

The representative topographic images (2D & 3D) of the Pt contacts on n-Al_{0.08}In_{0.08}Ga_{0.84}N film grown on sapphire substrate as deposited and after annealing treatment at 400–500 °C, for scanning square area of 10 × 10 μm, are shown in Figs. 2, 3 and 4a, b.

The depth histogram associated with Figs. 2, 3 and 4a, b of the Pt contacts on n-Al_{0.08}In_{0.08}Ga_{0.84}N film grown on sapphire substrate as deposited and after annealing treatment at 400–500 °C, are shown in Fig. 5a–c.

The graphical study of volume parameters (surface): *Vmp*, *Vvc*, *Vmc* & *Vvv* parameters based upon the Abbott curve calculated on the surface associated with Figs. 2, 3 and 4a, b are shown in Fig. 6a–c.

The curve of the material share provides important information about the condition of the surface in terms of its operational suitability. It is known that for the optimal functionality of the surface, it is required to be progressive or progressive-regressive.

The graphical study of *Sk* parameters associated with Figs. 2, 3 and 4a, b of the Pt contacts on n-Al_{0.08}In_{0.08}Ga_{0.84}N film grown on sapphire substrate as deposited and after annealing treatment at 400–500 °C, are shown in Fig. 7a–c.

The peak count histogram associated with Figs. 2, 3 and 4a, b of the Pt contacts on n-Al_{0.08}In_{0.08}Ga_{0.84}N film grown on sapphire substrate as deposited and after annealing treatment at 400–500 °C, are shown in Fig. 8a–c.

The graph of the calculated volume for surfaces (*V_ε*) drawn as a function of the scale (*ε*) (size of the structuring elements) associated with Figs. 2, 3 and 4 a, b of the Pt contacts on n-Al_{0.08}In_{0.08}Ga_{0.84}N film grown on sapphire substrate as deposited and after annealing treatment at 400–500 °C, are shown in Fig. 9a–c. The fractal dimension is calculated from the slope of that one of the two regression lines that corresponds best (i.e. the one out of the two regression lines whose correlation coefficient is nearer to 1 for a profile and nearer to 2 for a surface).

Table 1 presents a summary of the fractal dimensions *D_f* values, for scanning square areas of 10 × 10 μm², for Pt contacts on n-Al_{0.08}In_{0.08}Ga_{0.84}N film grown on sapphire substrate: (a) as deposited; (b) after annealing treatment at 400 °C; (c) after annealing treatment at 500 °C.

A summary of the statistical parameters results is presented in Table 2.

3 Results

Representative (2D & 3D) topographic images of the Pt contacts on n-Al_{0.08}In_{0.08}Ga_{0.84}N film grown on sapphire

Table 1 The fractal dimensions D_f values, for scanning square areas of $10 \times 10 \mu\text{m}^2$, for Pt contacts on n- $\text{Al}_{0.08}\text{In}_{0.08}\text{Ga}_{0.84}\text{N}$ film grown on sapphire substrate: (a) as deposited; (b) after annealing treatment at 400 °C; (c) after annealing treatment at 500 °C

No.	Samples	D_f
1	As deposited	2.25 ± 0.0001
2	After annealing treatment at 400 °C	2.04 ± 0.0001
3	After annealing treatment at 500 °C	2.15 ± 0.0001

* Statistically significant difference: $P < 0.05$

substrate as deposited and after annealing treatment at 400–500 °C, for 30 min respectively, for different scanning square areas, are shown in Figs. 2, 3 and 4a, b.

The 3D surface of all the samples is covered by nanoasperities (nano scaled protrusions and cavities which have irregular shapes, different sizes and separations) and a specific distribution due to the preparation processes, which is evident for the entire magnification range. These patterns clearly outline the fractal nature of the 3D surface.

Table 2 The statistical parameters for Pt contacts on n- $\text{Al}_{0.08}\text{In}_{0.08}\text{Ga}_{0.84}\text{N}$ film grown on sapphire substrate: (a) as deposited; (b) after annealing treatment at 400 °C; (c) after annealing treatment at 500 °C, according with ISO 25178

The statistical parameters	Symbol	Samples as deposited Values	Samples at 400 °C Values	Samples at 500 °C Values
Height parameters				
Root mean square height	Sq [nm]	6.71	8.61	10.2
Skewness	Ssk [–]	0.00688	–0.0209	0.262
Kurtosis	Sku [–]	2.13	2.03	2.01
Maximum peak height	Sp [nm]	19.7	20.0	22.2
Maximum pit height	Sv [nm]	12.8	17.5	17.4
Maximum height	Sz [nm]	32.5	37.5	39.5
Arithmetic mean height	Sa [nm]	5.59	7.33	8.67
Functional parameters				
Areal material ratio	Smr [%]	100	100	100
Inverse areal material ratio	Smc [nm]	8.90	11.5	15.0
Extreme peak height	Sxp [nm]	11.7	15.7	14.9
Spatial parameters				
Auto-correlation length	Sal [μm]	1.42	1.81	1.53
Texture-aspect ratio	Str [–]	0.278	0.357	0.296
Texture direction	Std [°]	0.352°	45.0°	115°
Hybrid parameters				
Root mean square gradient	Sdq [–]	0.0125	0.00376	0.0061
Developed interfacial area ratio	Sdr [%]	0.00785	0.000708	0.00186
Functional parameters (Volume)				
Material volume	Vm [$\mu\text{m}^3/\mu\text{m}^2$]	0.000215	0.000249	0.00029
Void volume	Vv [$\mu\text{m}^3/\mu\text{m}^2$]	0.00911	0.0118	0.0153
Peak material volume	Vmp [$\mu\text{m}^3/\mu\text{m}^2$]	0.000215	0.000249	0.00029
Core material volume	Vmc [$\mu\text{m}^3/\mu\text{m}^2$]	0.00741	0.0089	0.0104
Core void volume	Vvc [$\mu\text{m}^3/\mu\text{m}^2$]	0.00861	0.011	0.0147
Pit void volume	Vvv [$\mu\text{m}^3/\mu\text{m}^2$]	0.0005	0.000726	0.000627
Feature parameters				
Density of peaks	Spd [$1/\mu\text{m}^2$]	0.131	0.0101	0.0101
Arithmetic mean peak curvature	Spc [$1/\mu\text{m}$]	1.12	0.175	0.200
Ten point height	S10z [nm]	–	–	–
Five point peak height	S5p [nm]	4.06	–	–
Five point pit height	S5v [nm]	–	–	–
Mean dale area	Sda [μm^2]	–	–	–
Mean hill area	Sha [μm^2]	6.58	–	–
Mean dale volume	Sdv [μm^3]	–	–	–
Mean hill volume	Shv [μm^3]	0.00107	–	–

* Statistically significant difference: $P < 0.05$

A statistically significant difference ($P < 0.05$) was found for all fractal dimensions D_f values. Results of the fractal dimensions D_f values are summarized in Table 1.

The applied method reflected the correct values of the fractal dimensions D_f values (all with average \pm standard deviation) associated for the surface roughness of the thin films. These D_f values should be taken into account in the surface engineering design of Pt contacts on n-Al_{0.08}In_{0.08}Ga_{0.84}N film grown on sapphire substrate.

4 Discussion

The result of this study is an experimental method for better formation of Pt Schottky contacts grown on nanostructure Al_{0.08}In_{0.08}Ga_{0.84}N thin film grown by molecular beam epitaxy technique on sapphire substrate at annealing temperatures range of 300–500 °C. Their surface morphologies obtained from AFM images were subjected to statistical and fractal analysis to quantitatively investigate their structural properties.

In addition, the fractal nature of the real surface was investigated and the fractal dimensions D_f can be used as a quantitative factor to estimate of degree of fractality and understand their 3D roughness structures.

It can be concluded that the rearrangement of the Pt atoms with the increasing of temperature until 400 °C lead to create good metal–semiconductor interface. In addition, the annealing at 400 °C minimizes the effect of compressive stress and strain induced in the metal–semiconductor contact resulting from the normal heating process [6]. While, a high temperature annealing treatment leads to the degradation of the metal–semiconductor contacts.

The better surface morphology and high SBHs have been obtained for Pt/Al_{0.08}In_{0.08}Ga_{0.84}N contacts annealed at 400 °C. This relatively high temperature makes the samples is promising to optoelectronic devices operating in this temperature. High temperature annealing treatment leads to the degradation of the metal–semiconductor contacts therefore, it is not recommended.

The surface of all samples appeared relatively smooth, with very fine nano-asperities spread on the surface due to the preparation processes and is fractal in nature.

Coefficient of surface development S_{dr} and fractal dimension D_f has the lowest value for the sample annealed at 400 °C and the highest values for as deposited.

Results showed that fractal dimensions include important surface topography information and can also be used to investigate the Pt contacts on n-Al_{0.08}In_{0.08}Ga_{0.84}N film grown on sapphire substrate.

The nano-topography of the Pt contacts on n-Al_{0.08}In_{0.08}Ga_{0.84}N film grown on sapphire substrate can open a new perspective and allow new developments in studies on

electro-physical, mechanical, and thermal properties, from both theoretical and experimental perspectives.

The fractal analysis in correlation with the AFM data information provides a greater insight into surface roughness quality control and performance of Pt contacts on n-Al_{0.08}In_{0.08}Ga_{0.84}N film grown on sapphire substrate.

Acknowledgments The authors would like to thank Universiti Sains Malaysia USM, 11800 Penang, Malaysia for the financial support under 1001/PFIZIK/843088 grant and Science College, Thi-Qar University, Al-Muntazah, Nassiriya 00964, Iraq to conduct this research. Neither author has a financial or proprietary interest in any material or method mentioned

Appendix

The statistical parameters of 3D surface roughness, according with ISO 25178-2:2012 are defined as following [22].

a) Height parameters are a class of surface finish parameters that quantify the Z-axis perpendicular to the surface.

(Sq)—root mean square height is the standard deviation of the height distribution, or RMS surface roughness.

(Ssk)—Skewness is the third statistical moment, qualifying the symmetry of the height distribution. Negative skew indicates a predominance of valleys, while positive skew is seen on surfaces with peaks.

(Sku)—Kurtosis is the fourth statistical moment, qualifying the flatness of the height distribution. For spiky surfaces, $Sku > 3$; for bumpy surfaces, $Sku < 3$; perfectly random surfaces have kurtosis of 3.

(Sp)—Maximum peak height is the height between the highest peak and the mean plane.

(Sv)—Maximum pit height is the depth between the mean plane and the deepest valley.

(Sz)—Maximum height is the height between the highest peak and the deepest valley.

(Sa)—Arithmetical mean height is the mean surface roughness.

b) Functional parameters are calculated from the Abbott-Firestone curve obtained by the integration of height distribution on the whole surface.

(Smr)—Areal material ratio is the bearing area ratio at a given height. Ratio of the area of the material at a specified height c (cut level) to the evaluation area. The Smr(c) is expressed as a percentage. For the Smr parameter, the height c is counted by default from the mean plane.

(Smc)—Inverse areal material ratio is the height c at which a given areal material ratio p is satisfied. The height is calculated from the mean plane.

(Sxp)—Extreme peak height is the difference in height between q and p % material ratio. This parameter must be configured with two thresholds entered in %.

- c) Spatial parameters describe topographic characteristics based upon spectral analysis. They quantify the lateral information present on the X- and Y-axes of the surface.

(Sal)—Auto-correlation length is the horizontal distance of the autocorrelation function (t_x, t_y) which has the fastest decay to a specified value s , with $0 < s < 1$. The default value for s in the software is 0.2. This parameter expresses the content in wavelength of the surface. A high value indicates that the surface has mainly high wavelengths (low frequencies).

(Str)—Texture-aspect ratio is the ratio of the shortest decrease length at 0.2 from the autocorrelation, on the greatest length. This parameter has a result between 0 and 1. If the value is near 1, we can say that the surface is isotropic, i.e. has the same characteristics in all directions. If the value is near 0, the surface is anisotropic, i.e. has an oriented and/or periodical structure.

(Std)—Texture direction calculates the main angle for the texture of the surface, given by the maximum of the polar spectrum. This parameter has a meaning if Str is lower than 0.5.

- d) Hybrid parameters are a class of surface finish parameters that quantify the information present on the X-, Y- and Z-axes of the surface, i.e. those criteria that depend both on the amplitude and the spacing, such as slopes, curvatures, etc.

(Sdq)—Root mean square gradient is the root-mean-square slope of the surface.

(Sdr)—Developed interfacial area ratio is the ratio of the increment of the interfacial area of the scale limited surface within the definition area over the definition area. The developed surface indicates the complexity of the surface thanks to the comparison of the curvilinear surface and the support surface. A completely flat surface will have a Sdr near 0 %. A complex surface will have a Sdr of some percents.

- e) Functional volume parameters are typically used in tribological studies. They are calculated using the Abbott-Firestone curve (areal material ratio curve) calculated on the surface.

Vm(p)—Material volume is the volume of the material at a material ratio p (in %).

Vv(p)—Void volume is the volume of the voids at a material ratio p (in %).

Vmp—Peak material volume of the scale limited surface is the volume of material in the peaks, between 0 % material ratio and a material ratio p (in %), calculated in the zone above c_1 . $Vmp = Vm(p)$

Vmc—Core material volume of the scale limited surface is the volume of material in the core or kernel, between two material ratios p and q (in %), calculated in the zone between c_1 and c_2 . $Vmc = Vm(q) - Vm(p)$

Vvc—Core void volume of the scale limited surface is the volume of void in the core or kernel, between two material ratios p and q (in %), calculated in the zone between c_1 and c_2 . $Vvc = Vv(p) - Vv(q)$

Vvv—Pit void volume of the scale limited surface is the volume of void in the valleys, between a material ratio p (in %) and 100 % material ratio, calculated in the zone below c_2 . $Vvv = Vv(p)$

- f) Feature parameters are derived from the segmentation of a surface into motifs (hills and dales). Segmentation is carried out in accordance with the watersheds algorithm.

Spd—Density of peaks is the number of peaks per unit area.

Spc—Arithmetic mean peak curvature is the arithmetic mean of the principle curvatures of peaks within a definition area.

S10z—Ten point height is the average value of the heights of the five peaks with the largest global peak height added to the average value of the heights of the five pits with the largest global pit height, within the definition area. $S10z = S5p + S5v$

S5p—Five point peak height is the average value of the heights of the five peaks with the largest global peak height, within the definition area.

S5v—Five point pit height is the average value of the heights of the five pits with the largest global pit height, within the definition area.

Sda—Closed dale area is the average area of dales connected to the edge at height c .

Sha—Closed hill area is the average area of hills connected to the edge at height c .

Sdv—Closed dale volume is the average volume of dales connected to the edge at height c .

Shv—Closed hill volume is the average volume of hills connected to the edge at height c .

References

- J.R. Chen, T.S. Ko, P.Y. Su, T.C. Lu, H.C. Kuo, Y.K. Kuo, S.C. Wang, Numerical study on optimization of activelayer structures

- for GaN/AlGaIn multiple-quantum-well laser diodes. *J. Light-wave Technol.* **26**(17), 3155–3165 (2008)
2. R. Werner, M. Reinhardt, M. Emmerling, A. Forchel, V. Harle, A. Bazhenov, High-resolution patterning and characterization of optically pumped first-order GaN DFB lasers. *Physica E* **7**, 915–918 (2000)
 3. V. Rajagopal, M. Ravinandan, P. Koteswara, C.J. Choi, Effects of thermal annealing on the electrical and structural properties of Pt/Mo Schottky contacts on n-type GaN. *J. Mater. Sci.: Mater. Electron.* **20**(10), 1018–1025 (2009)
 4. J. Wang, D.G. Zhao, Y.P. Sun, L.H. Duan, Y.T. Wang, S.M. Zhang, H. Yang, S. Zhou, M. Wu, Thermal annealing behaviour of Pt on n-GaN Schottky contacts. *J. Phys. D Appl. Phys.* **36**(8), 1018–1022 (2003)
 5. C.L. Yu, C.H. Chen, S.J. Chang, P.C. Chang, GaN metal-semiconductor-metal ultraviolet photo detectors with Ir/Pt contact electrodes. *J. Electrochem. Soc.* **154**(2), J71–J72 (2007)
 6. Y.C. Lee, Z. Hassan, M.J. Abdullah, M.R. Hashim, K. Ibrahim, Dark current characteristics of thermally treated contacts on GaN-based ultraviolet photo detectors. *Microelectron. Eng.* **81**, 262–267 (2005)
 7. V.R. Reddy, M. Ravinandan, P.K. Rao, C.J. Choi, Electrical and structural properties of rapidly annealed Pd/Mo Schottky contacts on n-type GaN. *Semicond. Sci. Technol.* **23**(9), 095026 (2008)
 8. I. Vurgaftman, J.R. Meyer, L.R. Ram-Mohan, Band parameters for III-V compound semiconductors and their alloys. *J. Appl. Phys. Rev.* **89**(11), 5815–5875 (2001)
 9. A.J. Ghazai, H. Abu Hassan, Z. Hassan, A.S. Hussein, Effects of thermal annealing of Pt Schottky contacts on quaternary n-Al_{0.08}In_{0.08}Ga_{0.84}N thin film. *J. Optoelectron. Adv. M.* **6**(1–2), 324–326 (2012)
 10. B. Bhushan, *Introduction to Tribology*, 2nd edn. (John Wiley & Sons Ltd., New York, 2013)
 11. R.K. Leach, *Fundamental principles of engineering nanotechnology* (Elsevier Inc., Oxford, 2010)
 12. P. Sahoo, T. Barman, J.P. Davim, *Fractal Analysis in Machining* (Springer-Verlag, Heidelberg, 2011)
 13. S. Stach, J. Cybo, Multifractal description of fracture morphology: theoretical basis. *Mater. Charact.* **51**(1), 79–86 (2003)
 14. B.B. Mandelbrot, *The Fractal Geometry of Nature* (Freeman W. H, San Francisco, 1982)
 15. C.Q. Yuan, J. Li, X.P. Yan, Z. Peng, The use of the fractal description to characterize engineering surfaces and wear particles. *Wear* **255**(1–6), 315–326 (2003)
 16. B.N. Persson, O. Albohr, U. Tartaglino, A.I. Volokitin, E. Tosatti, On the nature of surface roughness with application to contact mechanics, sealing, rubber friction and adhesion. *J. Phys.: Condens. Matter* **17**(1), R1–R62 (2005)
 17. R.P. Yadav, S. Dwivedi, A.K. Mittal, M. Kumar, A.C. Pandey, Fractal and multi fractal analysis of LiF thin film surface. *Appl. Surf. Sci.* **261**, 547–553 (2012)
 18. Ş. Țălu, Mathematical methods used in monofractal and multifractal analysis for the processing of biological and medical data and images. *Anim. Biol. Anim. Husb.* **4**(1), 1–4 (2012)
 19. J. Schmähling, Statistical characterization of technical surface microstructure, Ph.D. Thesis (University of Heidelberg, Germany, 2006)
 20. S. Lou, X. Jiang, P.J. Scott, Application of the morphological alpha shape method to the extraction of topographical features from engineering surfaces. *Measurement* **46**(2), 1002–1008 (2013)
 21. MountainsMap[®] 7 Software (Digital Surf, Besançon, France). Available from: <http://www.digitalsurf.fr> (last accessed August 10, 2013)
 22. ISO 25178-2, Geometrical product specifications (GPS)—Surface texture: Areal—Part 2: Terms, definitions and surface texture parameters. Available from: <http://www.iso.org> (last accessed August 10, 2013)
 23. Product catalog. Available from: <http://www.nanosurf.com/> (last accessed August 10, 2013)
 24. Silicon AFM Probes. Available from: <http://www.vistaprobes.com> (last accessed August 10, 2013)
 25. SPIP, The Scanning Probe Image Processor, Denmark, 2013. Available from: <http://www.imagemet.com> (last accessed August 10, 2013)
 26. GraphPad InStat software, version 3.20 (GraphPad, San Diego, CA). Available from: <http://www.graphpad.com/instat/instat.htm> (last accessed August 10, 2013)